Petroleum 7 (2021) 142–151

Contents lists available at ScienceDirect

Petroleum

journal homepage: www.keaipublishing.com/en/journals/petlm

Nano-alumina based (alpha and gamma) drilling fluid system to stabilize high reactive shales

Ali Hassanzadeh, Afshar Alihosseini*, Majid Monajjemi, Mahdi Nazari-Sarem

Department of Chemical Engineering, Central Tehran Branch, Islamic Azad University, Tehran, Iran

A R T I C L E I N F O

Article history:
Received 16 April 2020
Received in revised form
28 June 2020
Accepted 9 July 2020

Keywords:
Water base fluid
nano-particle
Alpha alumina
Gamma alumina
Devices analyses

A B S T R A C T

Most of water based drilling fluids easily penetrate into shale formations and cause serious problems such as well instability, destruction of the formation, wall pipe folding and pipe adhesion. The present research aims to assess the effects of alumina nano-particles (alpha and gamma) on shale/clay stability due to the unique specifications of alumina (alpha and gamma) nano particles. The SEM, XRD, EDAX and AFM analyses of recovered shale samples indicate that the average size of alpha alumina nano-particles coating the shale surface and the pores existing in the shale is between 25 and 35 nm, whereas the average size of gamma alumina nano-particles coating the shale surface and the pores present in the shale is between 20 and 30 nm. In addition, samples recovered by nano-alpha reveal more porosity remained in the shale sample in comparison with the nano-gamma nano-sample. Furthermore, the results obtained from EDAX illustrate a suitable nano-gamma alumina over the recovered shale. The experiment with five types of drilling fluid without the presence of potassium chloride as an inhibitor salt designed. Thus, the water based drilling fluid containing nano-gamma alumina with less than 1 %wt was chosen as the best sample. Generally, the presence of alumina nano-particles optimizes the stability of formations containing ions like shale.

1. Introduction

Since shale formations are least stable and more susceptible to water, clay content and ionic compounds, they are identified as the most common and the most problematic drilling formations stone. Its permeability is negligible and it includes tiny pores (in nanometer) which are not affectively blocked by the solid particles of the common drilling solid particles. When a water based drilling fluid is exposed to shale, water absorption immediately occurs. It causes clay swelling. In fact, its tension and volume get increased. The tension enhancement leads to dwindle the formation tension. Finally, it brings about problems such as drill trapping, being laminated and the drilling pipe trapping [1]. Shale takes up almost 75% of drilled formations. More than 90% of the well instability problems are caused by very low permeability properties, high pore pressure of clay minerals and high capacity of CEC (cationic exchange capacity). The clay layers are swollen in touch with water. Lastly, the well wall becomes unstable and the shale is collapsed into the well. Shales are type of sedimentary rocks which are easily laminated. They also hold a high percentage of clay. They can be swollen, hydrated and fractured. While drilling through the shales, we are dealt with several problems such as well hole instability, wash outs, pipes trapping, high torque and directional drilling. Annually, 500 million dollars spent on dealing with well instability problems in shales. The water based muds are highly essential to guarantee the well stability in shales for the sake of environmental problems and the costs of oil based muds. In this regard, most of concerns are caused by the sensitivity of shales to water. The hydration of shales directs into resistance decrease and their fracture. Most of oil based muds are used to deal with problems concerning with shales drilling [2]. The oil based muds are mainly practiced in order to prevent well instability in shale formations. Regarding the drawbacks of this type of mud, researchers have been seeking to

* Corresponding author.
E-mail address: Afs.alihosseini@iauctb.ac.ir (A. Alihosseini).
Peer review under responsibility of Southwest Petroleum University.

Production and Hosting by Elsevier on behalf of KeAi

https://doi.org/10.1016/j.petlm.2020.07.003

substitute an optimized water based mud for the oil based mud in oil industry [3–5]. Recent studies indicate that the swell and collapse of shale are reduced through obstructing the entrances of porous surroundings, decreasing the shale permeability, drilling fluid, fluid and shale reaction. In consequence, different sizes of additives can improve these problems. The average sizes of particles in nano-fluids ranging from 10 nm to 100 nm or even smaller ones can diminish the low volume of nano-particles and prevent deposition and agglomeration. Furthermore, it reduces the costs necessary for the maintenance and transmission of these fluids. Notably, a relatively vast surface of these particles reduce the unbalance effects between the fluid and solid. As a result, it causes suspension stability. As the size of particles gets decreased, the relative surface of the thermal transmission gets larger. In fact, the thermal efficiency of floating particles, which is a function of thermal transmission surfaces, is increased by reducing the size of particles [6]. nano-particles can obstruct the shale pores and inhibit water flow into the shale. The nano-particles properly block the entrance of shale pores and prevent crossing the drilling fluid [7,8]. The effective presence and the influence of adding nano-particles to the water based drilling mud as well as its impact on water penetration into stiff and soft shale indicate that water penetration into shale will be reduced the most by nano-particles [9]. The drilling mud from four fields of Atoka shale and Mexico gulf were considered both in the presence and absence of nano-particles. It is economical to use nano-particles in marine drilling in order to control the well instability problems in shale formations [10,11]. The multi-purpose nano-additives help the well stability and reduce the formation decrease in water based fluid. It is estimated that millions of dollars are spent for the sake of the well instability. Indeed, the mildew is exposed to shale formations. Silica nano-particles are used as multi-mud additives to reduce limpid water, lubricate the mud, prevent shale swelling and stabilize the rheological properties. These nano-particles in different concentrations obstruct the pores of shale [12–14]. The laboratory studies on the effects of Fe_4O_3 on the rheological properties of the water based mud at various temperatures indicate that the viscosity and controlling water are kept during the operation. Accordingly, the Fe_4O_3 nano-particles of are able to keep the tension shear of fluids as the temperature at certain levels gets more than the shear amount [15–17] The multi-wall carbon nanotubes (CNTs) in water based drilling mud is used to improve the rheological properties of drilling fluid and the shale stability. Research shows that these nano-particles can help decrease fluid wasting. Therefore, it contributes to economize costs [18,19]. Analyzing the effect of Al_2O_3 nano-particle on rheological properties of the water based drilling fluids illustrates that the presence of Al_2O_3 nano-particles can stabilize the rheological properties at different temperatures. The Al_2O_3 nano-particles can keep the shear tension of the drilling fluid when the temperature is increased [20]. Moreover, these laboratory studies indicate that adding 1% of synthetic nano-particles of Aluminum oxide to the drilling fluid of plastic viscosity, decreases the effective viscosity, kinetic viscosity and yield point are diminished [21]. The nano-particle of aluminum oxide and silica/alumina are aimed at improving the rheological properties and reducing fluid losses. the research indicates that using nano-particle in suitable concentration can contribute to stabilize the rheological properties of drilling fluid. In fact, the filtration amount is reduced, whereas increasing the concentration of nano-particles decreases the amount of shear tension. The distribution of aluminum oxide through the drilling fluid can lead to enhance the thermal stability [22,23]. There are two main types of alumina groups called alpha and gamma. nano-particles are able to obstruct the shale pores and block the water flow into the shale. nano-particles can properly block the entrance of shale pores and prevent crossing the drilling fluid. The alpha type is stiffer and its surface area is less and known as corundum. Moreover, the alpha type holds a cubic structure. Thus, the alpha type includes less −OH groups. Indeed, this factor causes their pH difference. The softer type of alumina is gamma which is more porous. This factor expands the surface area. The gamma type holds rhombohedra structure. The solid phase of alpha type and the gamma type are porous. Henceforth, thermal conduction of alpha is higher. Shale recovery was assessed in comparison with control sample in micro scale. To investigate the properties of shale samples recovered by the alpha alumina and gamma alumina based drilling fluid, several analyses such as SEM[2], XRD[3], EDAX, AFM were performed. The most striking feature of this research is to evaluate scientific and practical viewpoints of nano-alpha alumina and nano-gama alumina while encountering reactive shale/clays. Also the comparison between alpha and gama phase of nano-alumina can remarkably assist researchers/drilling engineers while using these products.

2. Materials and methods

2.1. Materials

The properties of materials used in this work have been shown in Table 1. It is important to note that the necessary materials have been purchased from Sigma Aldridge Company.

2.2. Laboratorial equipment

In Table 2, the specifications of several devices used to analyze the samples have been shown. According to continuous calibration of these devices, their accuracy is acceptable. So, the analysis results are reliable.

2.3. The experiment method

In experimental section, the effect of common additives in water based drilling fluid properties such as rheological properties, filtration loss, shale/clay inhibition have been considered. The same evaluations have been done in the presence on alumina nano-particles in order to determine the effect of nano-particles on drilling fluid properties. According to the mixing procedure, each component was initially stirred for 10min (11000 rpm) to prepare the fluids. In the next step, the nano-additive powder was added to the fluid and mixed for at least 30 min. At the end, the fluid was stirred in a high rotation for 20 min in order to achieve a homogenous mixture. After the properties were measured, the fluids were put in hot roll at 250 °F temperature for 4hrs. Table 3 represents formulations related to water base drilling fluids.

Table 1
Features out the required materials.

Name of nanoparticle / Characteristics analysis	Alumina alpha	Alumina gamma
Density	3.97 g/m^3	3.89 g/m^3
Purity	99.9%	99%
APS	30 nm	20 nm
SSA	>100 m^2/g	<200 m^2/g
Appearance	White powder	White powder
Morphology	Nearly spherical	Nearly spherical

[1] scanning electron microscope.
[2] X-Ray Diffraction.

Table 2
Required laboratory equipment.

Company	Application	Device
Hamilton	preparing drilling fluids	Five-blade-stirrer
FANN 35	measuring the amount of fluid viscosity	Visco-meter
OFITE	Filtering under CO_2 pressure	the high temperature and high pressure filtration
FANN	At the pressure and temperature of psi 100	The high pressure filtration device APIT
3003 PTS	The detecting analysis of components using X ray diffraction	XRD
Zeiss₀ DSM-960A	Spectroscopy and 3D scanning from tiny structures	SEM

Table 3
The formulation of the Water base drilling fluid systems.

Additives	Application/Description	Unit	MUD #RR1	MUD #RR2	MUD #RR3	MUD #RR4
			Concentration	Concentration	Concentration	Concentration
Drill Water	Base Fluid	cc	335.8	335.1	335.8	335.1
nano-Alpha Alumina	nano-additive	lb/bbl	1.05	1.4	–	–
nano-Gama Alumina	nano-additive	lb/bbl	–	–	1.05	1.4
SODIUM CHLORIDE AC	Weighting agent	lb/bbl	25.2	25.1	25.2	25.1
KCL R-UPG	Weighting agent/Inhibitor	lb/bbl	0	0	0	0
CAUSTIC SODA	Ph control agent	lb/bbl	pH~9.5–10	pH~9.5–10	pH~9.5–10	pH~9.5–10
SODA ASH	Hardness control agent	lb/bbl	0.2	0.2	0.2	0.2
AMYLOSE B	Drilling starch/Fluid loss control agent	lb/bbl	5	5	5	5
PAC LV-TG	Fluid loss control agent	lb/bbl	1	1	1	1
BIO-XCD	XC-Polymer/Viscosifier	lb/bbl	1	1	1	1
BIOCIDE MP	Biocide/Bactericide	lb/bbl	a few	a few	a few	a few

2.4. The mineralogy of shale

Before and after recovery operation, the Scanning Electron Microscopy (SEM) is used to indicate the high porosity of shale/clay samples also confirm the inhibition of nano-particles in recovered shales. The presence of alpha alumina and gamma alumina nanoparticles is observed as a layer over the shale surface in analyses and images. Additionally, the EDAX analysis is used to detect all the elements existing in shale sample. The AFM analyses of recovered shales via nano-drilling fluid system with alpha alumina and gamma alumina are performed in order to illustrate inhibition mechanisms by this nano-drilling fluid system. Beside the physical mechanism of pore plugging, the AFM evaluation expresses another physical mechanism known as surface coating provided by nano-alumina (alpha and gamma) drilling fluids.

2.5. Shale recovery/inhibition method

The standard method of API RP 13I was applied to measure the shale inhibition amount. In this experiment, the drilling fluid was in connection with shale particles (placed between 5 and 10 mesh) for 4hrs in hot roll at 250 °F. The remained particles of shale were poured on mesh 35. Percentage of 20 gr of the primary shale remained on this mesh indicates the recovered shale. Obviously, as this number gets closer to 100, the inhibitor will be more efficient and stronger. The shales remained on mesh 35 are separated and dried at 140 °F of the extreme phase. Then, they are weighed so that they don't include any humidity. The amount of shale recovery is calculated as follow:

The amount of shale recovery% = [the mass of the recovered shale (gr)/ the primary shale mass (20gr)] × 100 (1)

3. Results and discussions

3.1. The mineralogy results of the Under-0 study shales

Fig. 1 represents the XRD analysis of shale samples to measure the amount of dominant minerals in shale samples. Table 4 displays the quality/quantity analysis of shale sample. The data obtained from this table figures out that the shale samples used in these experiments hold a percentage of montmorillonite more than 60% and they are very active. They are completely hydrated in a drilling water free from any inhibiting additive in less than 1 min. Other minerals like dolomite, calcite and quartz include 5%.

3.2. The SEM and EDAX analysis of the shale sample

Fig. 2 illustrates the recovered montmorillonite shale sample. Clearly, this image reveals several pores in the montmorillonite stone sample.

The EDAX analysis shows all the elements existing in the shale sample. As expected, Fig. 3 features out a high percentage of silica and aluminum in shale structure.

3.3. The SEM and EDAX analysis of recovered shale sample with nano-alumina (alpha and gamma) drilling fluid system

Fig. 4 displays the SEM analysis of shale samples recovered by nano-alumina (alpha and gamma) drilling fluid system with the concentration of 0.1% wt. Related images feature out the coating of shale surface by gamma alumina nano-particles. Notably, the average size of nano-particles coating shale surface and the pores in the shale is between 20 and 30 nm (X = 19.53 nm, Y = 16.67 nm, D = 25.67 nm). This size is equal to the average size of gamma and alpha alumina nano-particles.

The EDAX graph shows all the elements existing in the shale sample. As expected, in Fig. 5, the graph carries out that the weight percentage of aluminum is more than the blank sample.

3.4. The SEM and EDAX analysis of recovered shale sample by nano-alumina (alpha and gamma) drilling fluid system with concentration of 0.4%wt

Fig. 6 demonstrates the SEM analysis of the shales sample recovered by nano-alumina (alpha and gamma) drilling fluid system with concentration of 0.4%wt. remarkably, the average size of nano-particles coating shale surface and the pores in the shale is between 25 and 35 nm (X = 27.34 nm, Y = 30 nm, D = 40.59 nm).

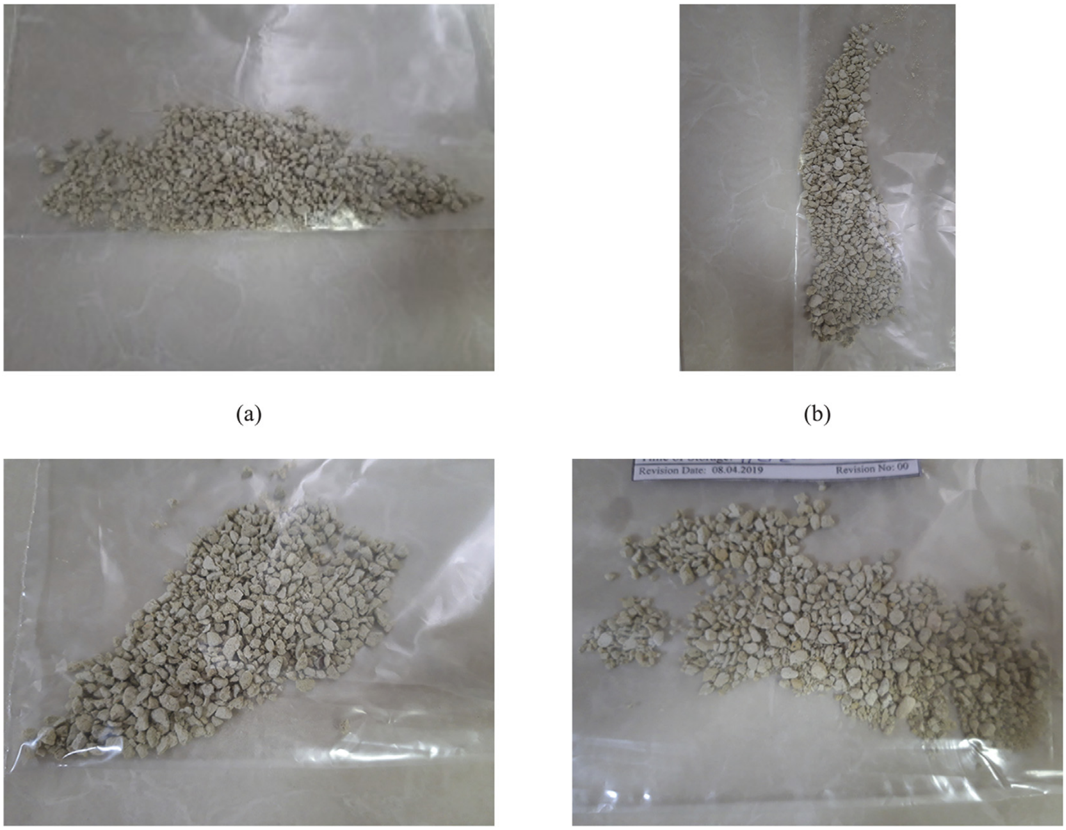

(a) (b) (c) (d)

Fig. 1. The shale samples recovered by nano-drilling fluid system after hot rolling.

Table 4
The quality/quantity analysis of shale stone sample.

Combination percentage (%)	Formulation	the formation phase
61	$Ca_{0.2}(Al,Mg)_2Si_4O_{10}(OH)_2$, xH_2O	montmorillonite (13–0135)
13	SiO_2	quartz (33–1161)
12	SiO_2	christobalite (39–1425)
5	$CaCO_3$	calcite (05–0586)
4	$CaMg(CO_3)_2$	volomite (36–0426)
1	$CaSO_4$, $2H_2O$	gypsum (33–0311)

This size is equal to the average size of alpha and gamma alumina nano-particles. Moreover, more pores are remained in the shale sample in comparison with nano-gamma alumina sample.

The EDAX analysis indicates all the elements existing in the shale sample. Fig. 7. Shows the EDAX analyses of shale sample recovered by nano-drilling fluid system with nano-gama alumina with the concentration of 0.4wt. As expected, in Fig. 7, the graph features out that the weight percentage of aluminum is more than the blank sample. However, the weight percentage of aluminum is less than that of Nano gamma alumina. In related spectrum, some Cl^- has been observed. This observed Cl^- originates from the potassium chloride solution which has been used for the final wash of the shale sample (according to the API-RP 13 I standard).

3.5. The AFM analysis of shale sample (blank sample)

Fig. 8 shows the 2-dimension (2D) analysis of the blank sample (the blank water base drilling fluid) in the absence of alpha alumina and gamma alumina nano-particles. The micro-metric dimensions of blank sample in AFM analysis have been clearly indicated. Fig. 9 is 3-dimensional image (3D) of blank sample.

3.6. The AFM analysis of recovered shale by nano-alumina drilling fluid system

Fig. 10 shows the 2D images of AFM of shale sample recovered by nano-alumina (alpha and gamma) drilling fluid systems. These analyses have been done in various resolutions ranging from 5mdt to 40 mdt. As indicated by the images, the measurements related to the AFM software displays the nano-metric dimensions of particles. Fig. 11 discloses the 3D images of AFM analysis of the shale samples recovered by nano-alumina (alpha and gamma) drilling fluid system.

A comparison between 3D images of the blank sample and the shale sample recovered by nano-alumina (alpha and gamma) drilling fluid system clearly indicates that the appearance of the shale surface has been changed which can be observed in all analysis. Hence, the peaks illustrate the proper formation of nano-layers from alpha alumina on shale surface.

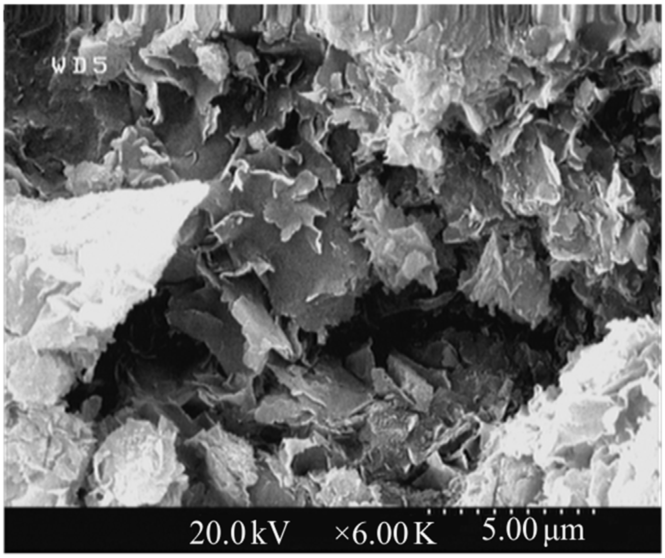

Fig. 2. The recovered montmorillonite shale stone sample.

3.7. The AFM analysis of the recovered shale by gamma alumina drilling fluid system

Fig. 12 shows 2D images of AFM analysis of the shale sample recovered by nano-alumina (gamma) drilling fluid system. These analyses have been done in different resolutions ranging from 5mdt to 40 mdt. As indicated by images, the measurements related to the AFM analysis shows the nano-metric dimensions of particles. Also Fig. 13 displays the 3D images of AFM analysis of the shale sample recovered by gamma alumina drilling fluid system. The white dots observed in these images are in Nano metric diameters and 3D images of AFM analysis show the proper formation of nano-layers from gamma alumina on shale surface.

A comparison between 3D images of blank sample and the shale sample recovered by nano-alumina (gamma) drilling fluid system indicates clearly that the morphology of the shale surface has been changed which can be observed in all images. Hence, the peaks illustrate the proper formation of nano-layers from gamma alumina on shale surface. Fig. 14 indicates the Nano layer profile of alpha alumina on the recovered shale. The shale sample recovered by nano-alumina drilling fluid system profile by nano-alumina drilling fluid system are indicated in Fig. 14. The profile shows that layer

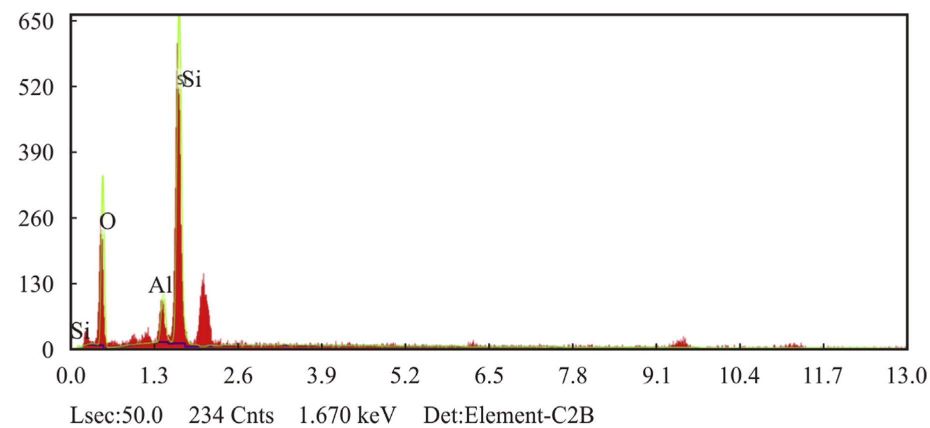

Fig. 3. EDAX analysis of the unrecovered shale stone sample.

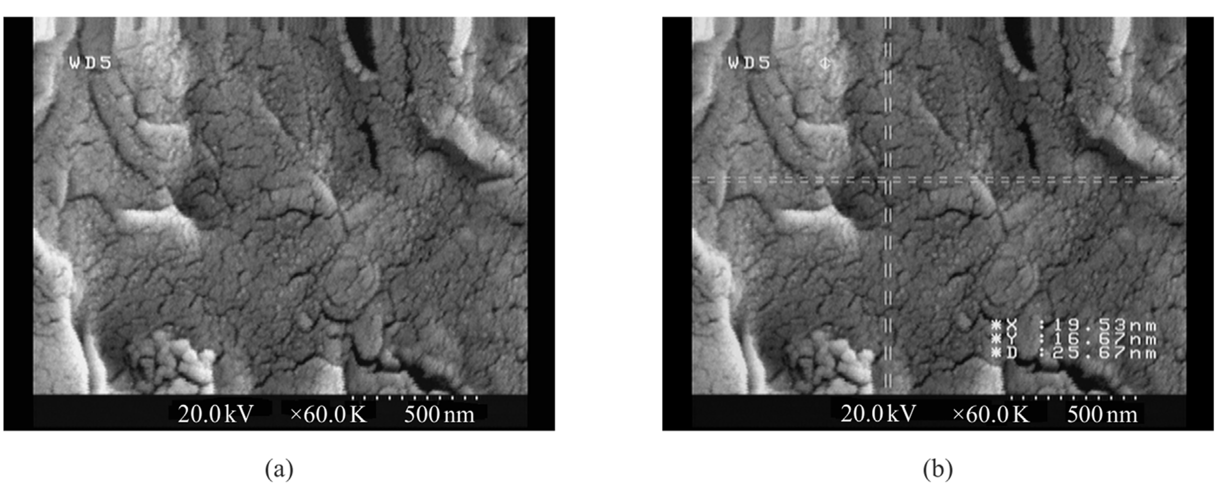

Fig. 4. SEM images of shale sample recovered by nano-alumina (alpha and gamma) drilling fluid system with concentration of 0.1%wt.

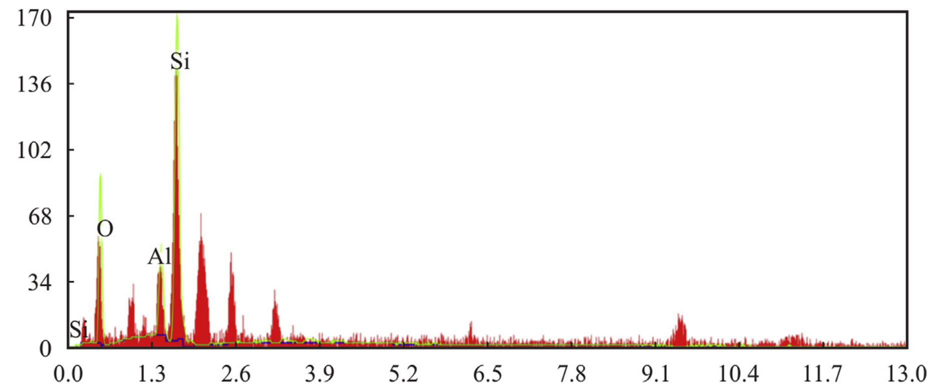

Fig. 5. EDAX analysis of shale samples recovered by nano-alumina (alpha and gamma) drilling fluid system with concentration of 0.1%wt.

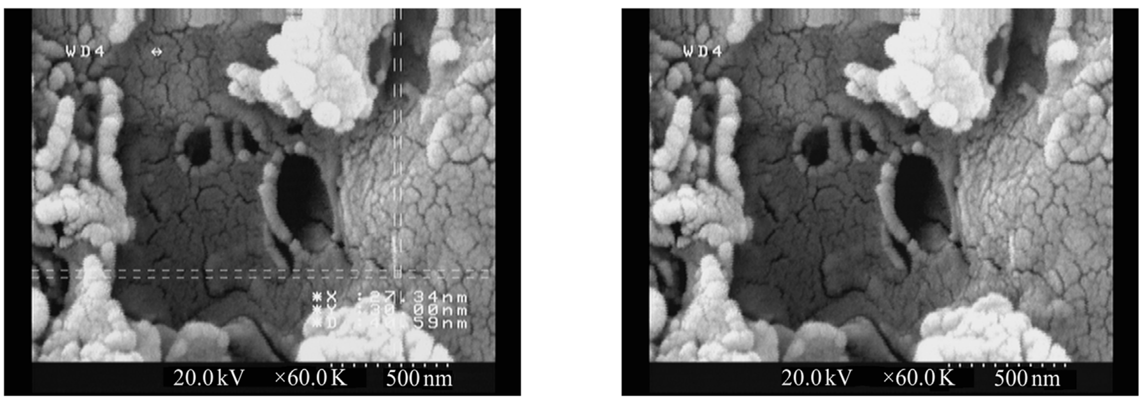

(a) (b)

Fig. 6. SEM analysis of shale sample recovered by nano-alumina (alpha and gamma) drilling fluid system with concentration of 0.4%wt.

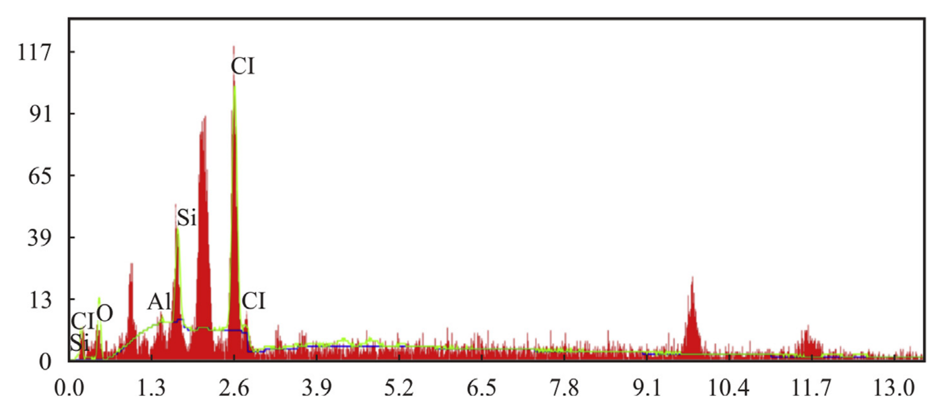

Fig. 7. EDAX analysis of shale sample recovered by nano-alumina (alpha and gamma) drilling fluid system with concentration of 0.4%wt.

size ranges are between 300 and 7550 nm and/or 0.3–0.75 μm. The enhancement of this layer thickness divulges that the alumina nano-particles have been formed as a single nano-layer on the blank sample layer.

As indicated in 3D images, the gamma alumina nano-layer can be formed over on the shale surface. Fig. 15 indicates the Nano layer profile of gama alumina on the recovered shale. According to this profile, nano-alumina layer size is ranged from 320 to 450 nm or from 0.32 to 0.45. The increase of the layer thickness expresses that the gamma alumina nano-particles are formed as single nano-layer on the control sample.

4. Conclusions

The present study has investigated the inhibition effects of modified Water based fluid with nano-alpha alumina and nano-gamma alumina based fluid for the stability of shale formation. According to the achieved data, the following results have been concluded. The alpha and gamma alumina can properly coat the shale surfaces in comparison with the unrecovered shale sample. SEM images indicate the pore plugging also surface coating mechanisms for shale inhibition by alpha and gama alumina nano-particles. Besides SEM, AFM confirms nano-layer formation on

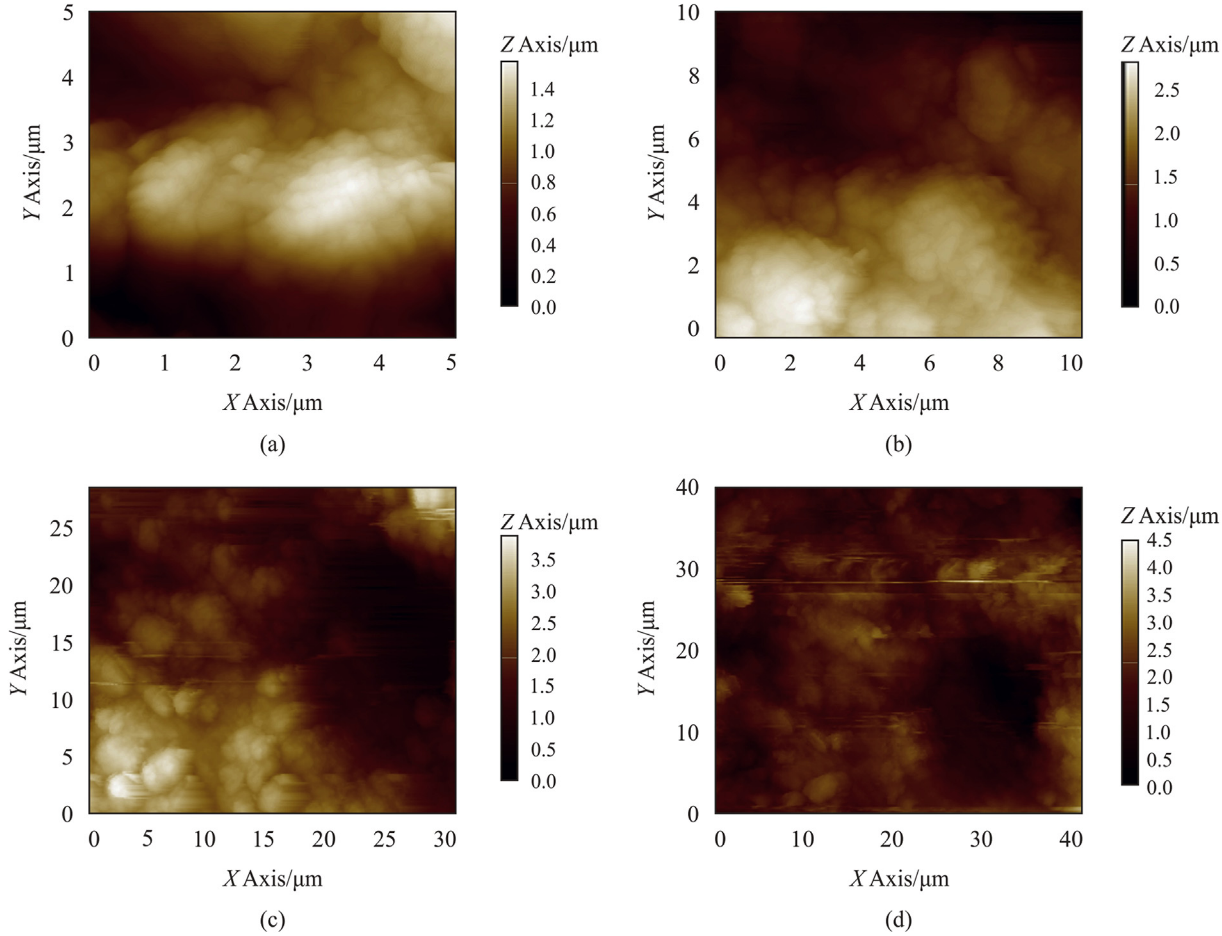

Fig. 8. AFM analysis for 2D of blank sample in the magnitude of 5, 10, 30, 40 mdt.

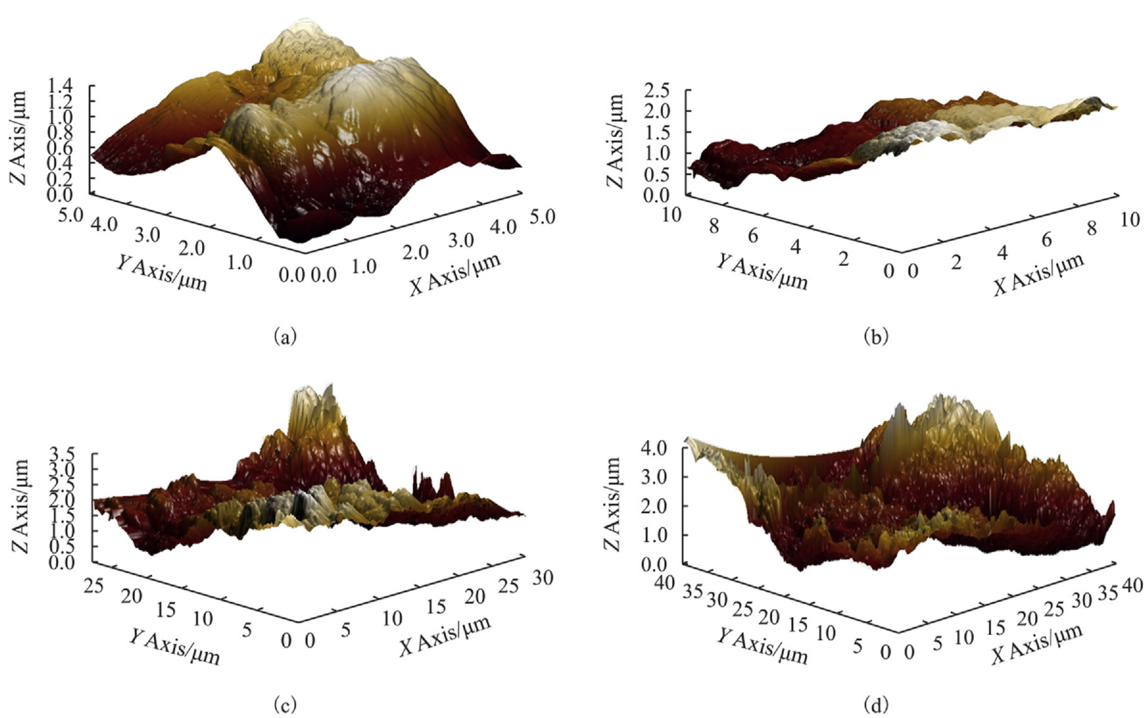

Fig. 9. AFM analysis of 3D of blank sample in the magnitude of 5, 10, 30, 40 mdt.

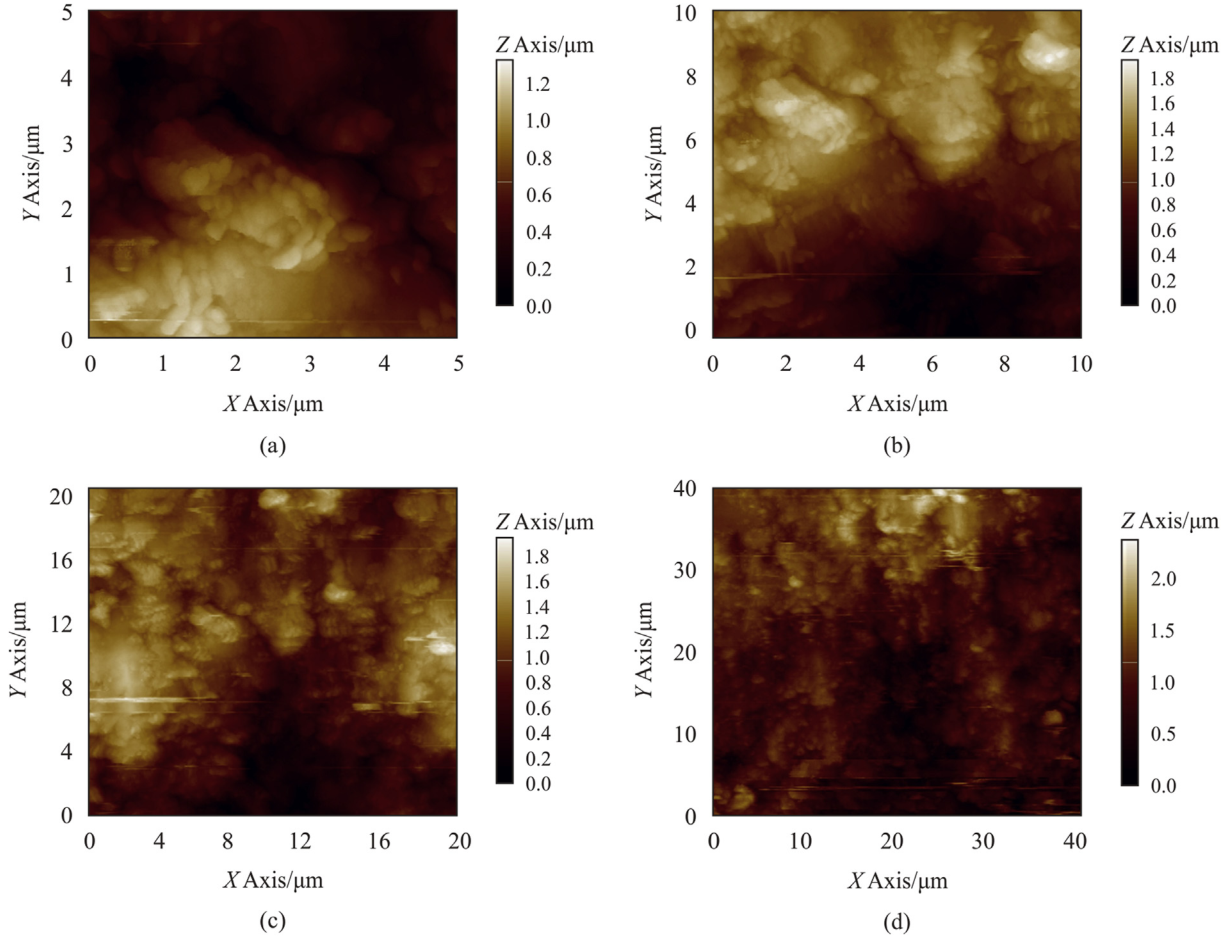

Fig. 10. AFM analysis for 2D of the shale sample recovered by nano-alumina in the magnitude of 5, 10, 30, 40 mdt.

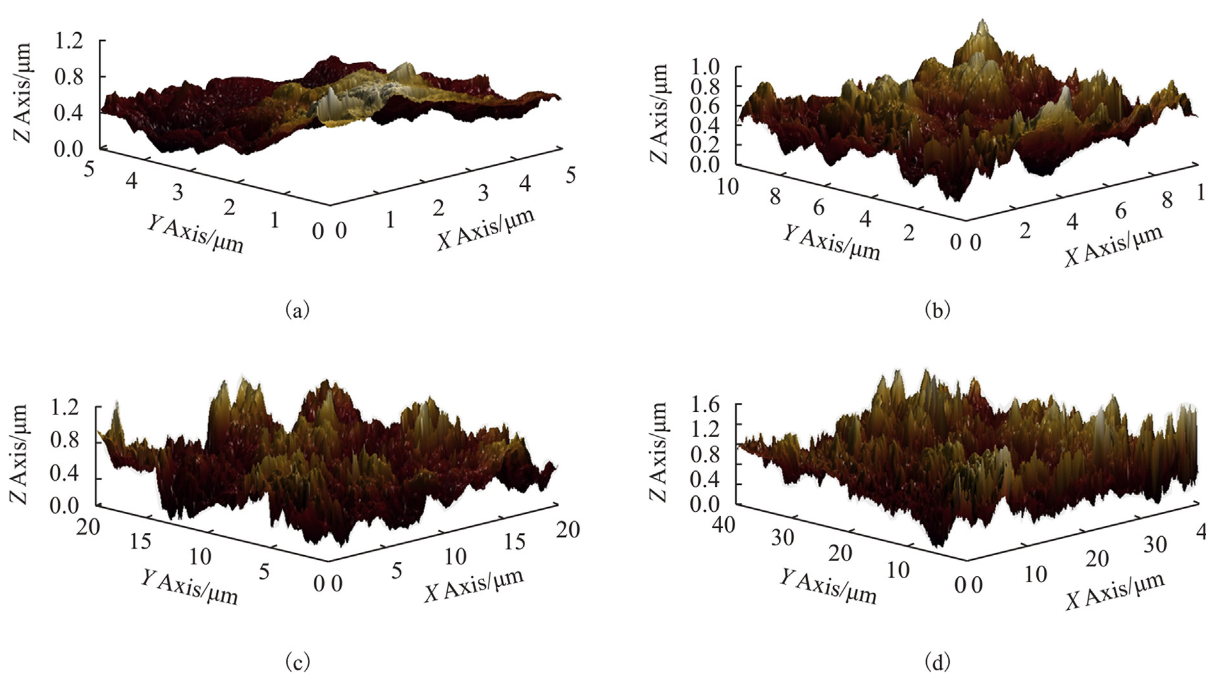

Fig. 11. AFM analysis for 3D of shale sample recovered by nano-alumina in the magnitude of 5, 10, 30, 40 mdt.

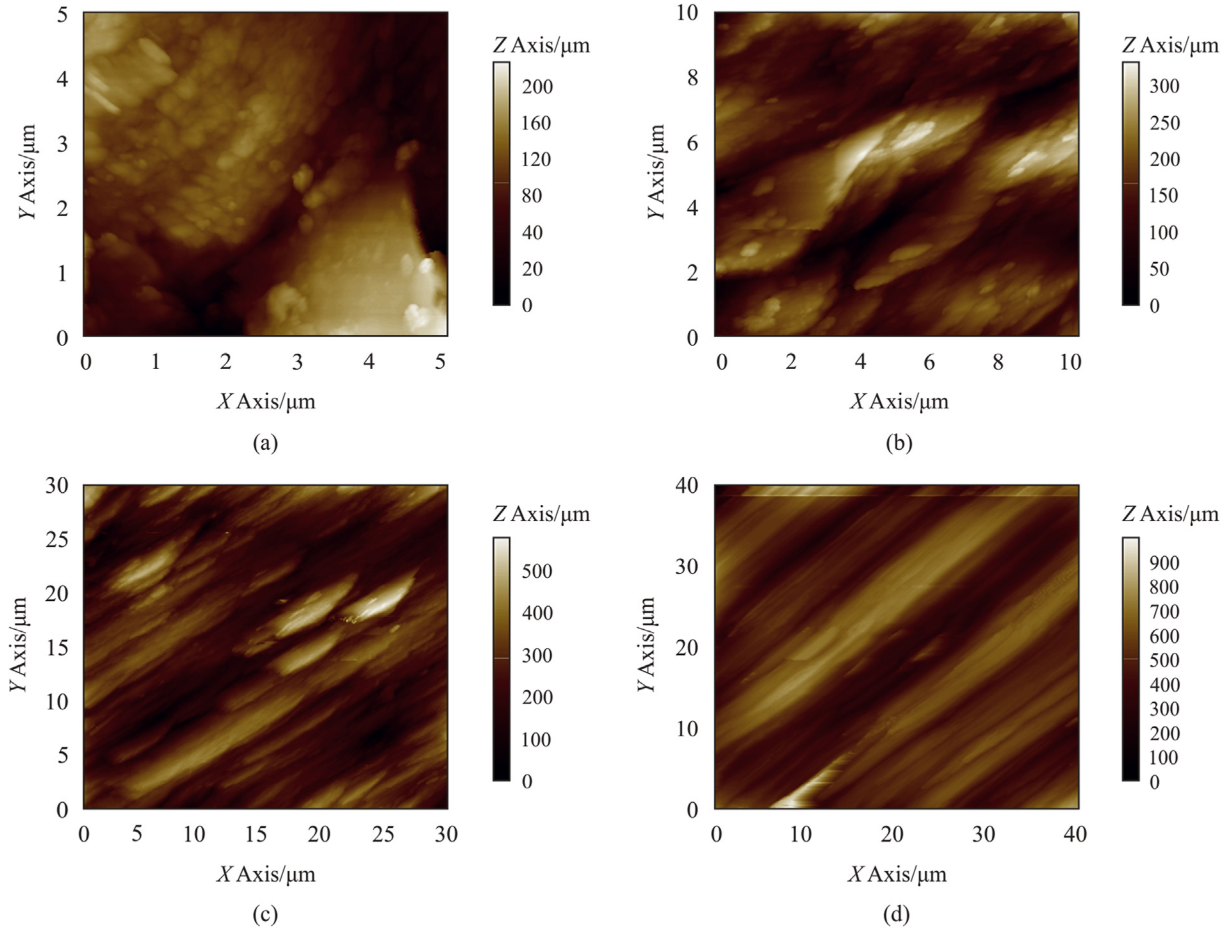

Fig. 12. AFM analysis for 2D of the shale sampleS recovered by gamma alumina in the magnitude of 5, 10, 30, 40 mdt.

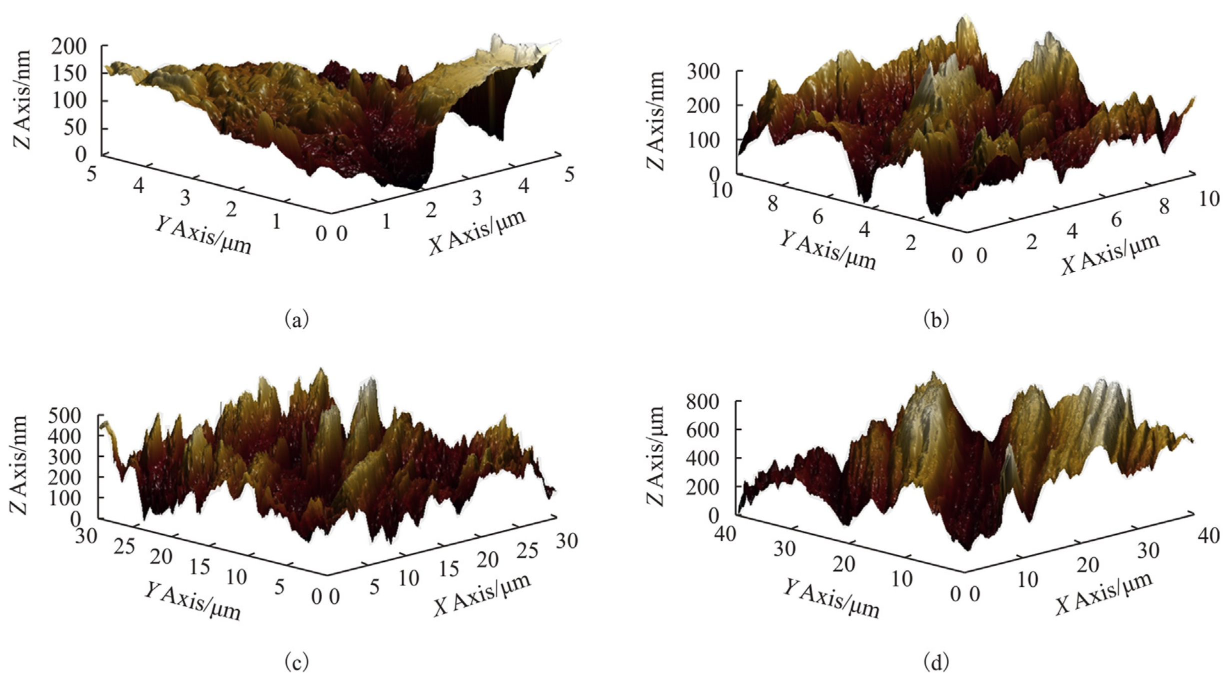

Fig. 13. AFM analysis for 3D of the shale sample recovered by gamma alumina in the magnitude of 5, 10, 30, 40 mdt.

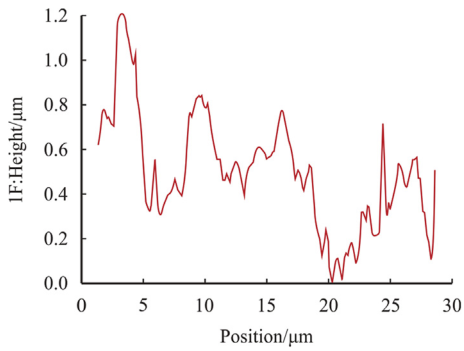

Fig. 14. Profile of alpha alumina nano-layer in the magnitude of 30mdt.

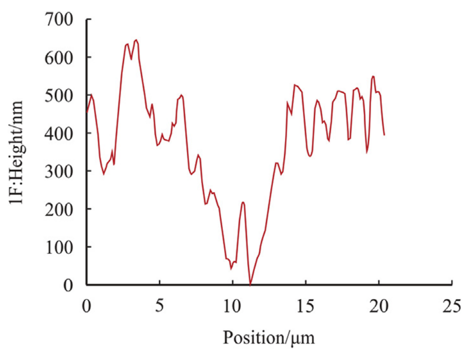

Fig. 15. Profile of gamma alumina nano-particles in the magnitude of 30mdt.

cuttings (shale samples). With the same concentration (0.4%wt) of both nano-alpha and nano-gama alumina, nano-gama alumina has the highest shale recovery/inhibition in com. The AFM analyses evaluation expresses another physical mechanism known as surface coating and shale inhibiting mechanisms. The 3D images of AFM analysis feature out that using nano-alumina (alpha and gama) can change the cuttings morphology and makes it more homogenous. Comparing the thickness profile of recovered shale samples with both nano-alpha and nano-gama alumina. Indicates multi- nano-metric layers of alpha alumina and gamma alumina on shale surfaces.

Declaration of competing interests

The authors declare that they have no known competing financial interests or personal relationships that could have appeared to influence the work reported in this paper.

References

[1] Y. Steve, Graphene-based material for shale stabilization and method of use U.S. Patent Application, 2011. No.13/877 page 852.
[2] T. Sensoy, M.E. Chenevert, M. Sharma, Minimizing water invasion in shales using Nanoparticles, in: SPE Annual Technical Conference and Exhibition, Society of Petroleum Engineers, USA, 2009. Pag16.
[3] k. Tookallo, J. Heidarian, Drilling Fluid- Nanodrilling Fluid, Scholar press, 2018.
[4] M. Pour Faraj Qajari, S.A. Tabatabaeinejad, M. Emami, Experimental investigation of the effect of nanoparticle size and concentration on the shale stability of an Iranian reservoir, in: First International Oil Conference, Iran, 2012 (in Persian).
[5] T. Sensoy, M.E. Chenevert, M.M. Sharma, Minimizing water invasion in shale using nanoparticles, PE (2009) 124429.
[6] H. Pham, Q.P. Nguyen, Effect of silica Nanoparticles on clay swelling and Water stability of Nanoparticle dispersions, J. Nano Res. 16 (1) (2014) 2137.
[7] S. Taraghikhah, M. Kalhor, N.K. Tahmasbi, Multifunctional Nanoadditive in water based drilling fluid for improving shale stability, in: International Petroleum Technology Conference, 2015.
[8] M. Petar, G.M. Nediljka, P. Borivoje, M. Igor, The influence of TiO2 and SiO2 Nanoparticles on filtration properties of drilling muds, Mining-Geology-Petroleum Engineering Bulletin (2019) 1–12.
[9] E.M. Amarfio, M. Abdulkadir, Effect of Fe4O3 nanoparticles on the rheological properties of water based mud, J. Phys. Sci. Appl. 5 (6) (2015) 415–422.
[10] E.M. Amarfio, M. Abdulkadir, Effect of Al2O3 Nanoparticles on the rheological properties of water based mud, Int. J. Sci. Eng. Appl. 5 (2016) 7–11.
[11] S. Hosseini, F. Farahbod, G. Zargar, The study of effective of added aluminum oxide nano particles to the drilling fluid: the evaluation of two synthesis methods, J. Petrol Environ. Biotechnol. 7 (3) (2016) 1–5.
[12] A. AliHosseini, S.H. Hosseini, A.R. Abbas Zadeh, Study of compress strength and time setting of concrete by additives of silica fume and Nano silica, Asian J. Chem. 24 (2) (2012) 903.
[13] Andres M. Oleas, E. Collins, Martin E. Mukul M. Sharma, Entrance pressure of oil-based mud into shale: effect of shale, water activity, and mud properties, in: SPE 116364, Presentation at the SPE Annual Technical Conference and Exhibition, Denver, 21–24 September, 2008.
[14] E. Kasiralvalad, The great potential of Nanomaterials in drilling & drilling fluid applications, Int. J. Nano Dimens. (IJND) 5 (5) (2011) 463.
[15] O. Contreras, G. Hareland, M. Husein, R. Nygaard, M. Al-Saba, Application of in-house prepared Nanoparticles as filtration control additive to reduce formation damage, in: International Symposium and Exhibition on Formation Damage Control. Society of Petroleum Engineers., Louisiana. USA, 2014.
[16] V. Bolis, G. Cerrato, G. Magnacca, C. Morterra, Surface acidity of metal oxides.Combined micro calorimetric and IR-spectroscopic studies of variously dehydrated systems, J. Therm. acta 312 (1998) 63–77.
[17] G. Paglia, C.E. Buckley, A.L. Rohl, R.D. Hart, K. Winter, A.J. Studer, B.A. Hunte, J.V. Hanna, Boehmite derived γ-alumina system. 1. Structural evolution with temperature, with the identification and structural determination of a new transition phase, γ'- Alumina, Chem. Mater. 16 (2004) 220–236.
[18] J. Abdo, M.D. Haneef, Clay Nanoparticles modified drilling fluids for drilling of deep hydrocarbon wells, Appl. Clay Sci. 86 (2013) 76–82.
[19] H. Mao, Z. Qiu, Z. Shen, W. Huang, Hydrophobic associated polymer based silica Nanoparticles composite with core-shell structure as a filtrate reducer for drilling fluid at ultra-high temperature, J. Petrol. Sci. Eng. 129 (2015) 1–14.
[20] J.G. Xu, Z. Qiu, X. Zhao, W. Huang, Hydrophobic modified polymer based silica Nanocomposite for improving shale stability in water-based drilling fluids, J. Petrol. Sci. Eng. 153 (2017) 325–330.
[21] O. Razavi, A.K. Vajargah, E. van Oort, M. Aldin, S. Govindarajan, Optimum particle size distribution design for lost circulation control and wellbore strengthening, J. Nat. Gas Sci. Eng. 35 (2016) 836–850.
[22] Y. Kang, J. She, H. Zhang, L. You, M. Song, Strengthening shale wellbore with silica Nanoparticles drilling fluid, J. Petrol. (2016) 2 189–195.
[23] S.R. Smith, R. Rafati, A. Sharifi haddad, A. Cooper, H. Hamidi, Application of Aluminium oxide Nanoparticles to enhance rheological and filtration properties of water based muds at HPHT conditions, Colloid. Surface. Physicochem. Eng. Aspect. 537 (2018) 361–371.